Pediatr Radiol (2015) 45:1761–1770
DOI 10.1007/s00247-015-3401-1

ORIGINAL ARTICLE

Coronary artery visibility in free-breathing young children on non-gated chest CT: impact of temporal resolution

Alexandre Bridoux[1] · Antoine Hutt[1] · Jean-Baptiste Faivre[1] · Thomas Flohr[2] · Alain Duhamel[3] · Julien Pagniez[1] · Jacques Remy[1] · Martine Remy-Jardin[1]

Received: 27 November 2014 / Revised: 8 April 2015 / Accepted: 1 June 2015 / Published online: 21 August 2015

Abstract
Background Dual-source CT allows scanning of the chest with high pitch and high temporal resolution, which can improve the detection of proximal coronary arteries in infants and young children when scanned without general anesthesia, sedation or beta-blockade.
Objective To compare coronary artery visibility between higher and standard temporal resolution.
Materials and methods We analyzed CT images in 93 children who underwent a standard chest CT angiographic examination with reconstruction of images with a temporal resolution of 75 ms (group 1) and 140 ms (group 2).
Results The percentage of detected coronary segments was higher in group 1 than in group 2 when considering all segments (group 1: 27%; group 2: 24%; P=0.0004) and proximal segments (group 1: 37%; group 2: 32%; P=0.0006). In both groups, the highest rates of detection were observed for the left main coronary artery (S1) (group 1: 65%; group 2: 58%) and proximal left anterior descending coronary artery (S2) (group 1: 43%; group 2: 42%). Higher rates of detection were seen in group 1 for the left main coronary artery (P=0.03), proximal right coronary artery (P=0.01), proximal segments of the left coronary artery (P=0.02) and proximal segments of the left and right coronary arteries (P=0.0006).
Conclusion Higher temporal resolution improved the visibility of proximal coronary arteries in pediatric chest CT.

Keywords Chest · Children · Computed tomography · Computed tomographic angiography · Dual-source computed tomography · Temporal resolution

✉ Martine Remy-Jardin
martine.remy@chru-lille.fr

[1] Department of Thoracic Imaging, Hospital Calmette (EA 2694), CHRU et Université de Lille, Boulevard Jules Leclerq, 59037 Lille Cedex, France

[2] Department of Research & Development in CT, Siemens Healthcare, Forchheim, Germany

[3] Department of Biostatistics, Université de Lille, Lille, France

Introduction

The introduction of dual-source CT technology has allowed standard chest CT examinations with high pitch and high temporal resolution. These scanning conditions are made possible by the simultaneous use of the two tubes of the dual-source CT system, which allows coverage of the entire thorax in very short scanning times but also allows scanning of patients with a 75-ms temporal resolution [1]. The short examination times have been shown to be beneficial for all categories of patients, especially those unable to follow breathing instructions or hold still during examinations. Adult populations have been reported to be scanned while freely breathing without deterioration of the diagnostic value of chest CT examinations [2, 3]. In pediatric populations, short examination times obviate the need for sedation or controlled ventilation for the examination of infants, small or uncooperative children [4]. Scanning patients with a high temporal resolution opens the field of examining thoracic cardiovascular structures in conditions approaching those achievable with electrocardiographic (ECG)-gated modes.

In adults undergoing chest or thoracoabdominal examinations, the aortic root, the whole aorta and the proximal segments of the coronary arteries have recently been shown to be accessible on non-ECG-synchronized CT examinations [5–10]. In pediatric populations, a single study investigated the accuracy and safety of non-gated, high-pitch modes in

young children with complex congenital heart disease [11]. However these examinations were performed under sedation and the scan range was always tailored to answer a specific clinical question. To our knowledge, the impact of temporal resolution has not been investigated in the conditions of routine pediatric chest CT examinations. To address this issue, we investigated a population of infants and young children who were scanned without general anesthesia, sedation or beta-blockade, and we analyzed the rate of detection of coronary arteries according to the temporal resolution of data acquisitions. Our hypothesis was that proximal coronary artery segments would be more sharply analyzed on images with optimized temporal resolution.

Materials and methods

Study sample

Our study group included consecutive children referred for a chest CT examination in our department who fulfilled the following criteria: (1) age ≤4 years; (2) had chest CT angiography obtained in a variety of indications, except congenital heart disease (we excluded congenital heart disease because first, state-of-the-art evaluation of congenital heart disease requires an ECG-synchronized mode, and second, the evaluation of the rate of coronary artery detection assumed a modal origin of these vessels); (3) had non-ECG synchronized chest CT angiography obtained with dual-source single-energy spiral acquisition and a pitch of 2 (i.e. standard protocol for pediatric chest CT examinations in our department) on the same CT unit; (4) availability of raw data for reconstruction of images with optimized and standard temporal resolution as further described (because of the clinical research activities of the department, raw data are systematically stored on external disks during clinical activities).

All investigations in the study sample were part of standard care. Retrospective reconstruction of images and subsequent analysis were undertaken with approval of our institutional review board and waiver of relatives' informed consent according to national regulations.

CT protocol

All children were examined using a second-generation dual-source CT system (Somatom Definition Flash; Siemens Healthcare, Forchheim, Germany) with a non-ECG-gated, dual-source, single-energy spiral acquisition using the following parameters: slice collimation 2×128×0.6 mm using a z-flying focal spot technique, pitch 2.0, rotation time 280 ms, 70 kV, 80 mAs. Because of the small size of the thorax in the study patients, the automatic modulation of tube current was not activated. Children were scanned while freely breathing, without sedation or general anesthesia; no oral or intravenous beta-blocker was administered. In order to scan quiet children, each examination was supervised by a pediatric nurse practitioner.

Iohexol 240 mg/ml or 300 mg/ml (Omnipaque; GE Healthcare SAS, Vélizy-Villacoublay, France), was manually injected with a total volume of 2 ml/kg body weight. Data acquisition was triggered at the end of the injection. CT angiography was performed without complication in all patients; there was no extravasation of contrast material at the injection site; there was no systemic reaction to the contrast material.

Image reconstruction

Each dataset was reconstructed twice. The first reconstruction used all data available per image from both tubes; this reconstruction corresponded to the commercially implemented dual-source reconstruction system with a temporal resolution of 140 ms. The second reconstruction discarded some data from both tubes to reconstruct images with a temporal resolution of 75 ms. A detailed description of the reconstruction process is given in the Appendix. The images acquired with a temporal resolution of 75 ms corresponded to images with optimized temporal resolution; we designated these images as group 1 images. The images acquired with a temporal resolution of 140 ms corresponded to images with standard temporal resolution and were designated as group 2 images. Group 1 and group 2 transverse CT images were reconstructed with a slice thickness of 0.75 mm, an increment of 0.5 mm, using a medium smooth-tissue convolution kernel with sinogram-affirmed iterative reconstruction (SAFIRE) (I26f). All images were anonymized and transferred to an external workstation (Multi-Modality Workplace; Siemens Healthcare, Forchheim, Germany).

CT parameters analyzed

Characteristics of chest CT examinations

For each examination, we recorded the dose-length product (mGy.cm) and calculated the effective dose (mSv), estimated from the dose-length product as previously described [12]. The recorded dose-length product was multiplied by 2 because on the machine used for the study the dose-length product for the body surface area was given on a 32-cm phantom and was half the dose-length product value found on a 16-cm phantom for the same acquisition. We used the following dose-length product conversion coefficients for a 16-cm phantom: 0.039 until 4 months of age, 0.026 at 4 months to 1 year of age, and 0.018 at 1–6 years of age. The objective image quality of group 1 and group 2 chest CT angiograms was assessed by measurements of the attenuation value, noise and calculation of the signal-to-noise ratio at the level of the

ascending aorta and pulmonary trunk. The attenuation was measured in the middle of the ascending aorta and the pulmonary trunk in a 1-cm^2 circular region of interest. The noise was defined as the standard deviation of the attenuation value, and the signal-to-noise ratio was calculated as the ratio of the attenuation value and the noise [13].

Visibility of coronary arteries

Coronary arteries were divided into nine segments including: (S1) the left main coronary artery, (S2) the proximal, (S3) middle and (S4) distal left anterior descending artery, the (S5) proximal and (S6) distal left circumflex artery, and the (S7) proximal, (S8) middle and (S9) distal right coronary artery. Segments of coronary arteries were equally divided for each coronary artery by length (1/3 of the total length for the right coronary artery or the left anterior descending artery; 1/2 of the total length for the left circumflex artery, as proposed in previous studies [13, 14]). Among these nine segments, four segments (S1, S2, S5 and S7) were defined as proximal, two segments (S3 and S8) as middle and three segments (S4, S6 and S9) as distal coronary segments. The visibility of proximal and mid-segments (i.e. six segments per patient) was the primary investigation of the present study. A five-grade scoring system was used to assess artery visibility on group 1 and group 2 images [13–15]. Grade 5 was a clear visualization without any motion artifacts; grade 4, mild motion artifacts but still with high diagnostic confidence; grade 3, obvious blurring, moderate diagnostic confidence; grade 2, identified but equivocal and may simulate other structures; grade 1, severe motion artifacts, no coronary segment visualized. Grades 1 and 2 were considered "not detected." Grades 3, 4 and 5 were considered "detected"; they are illustrated in Fig. 1. Paired images of each child were compared to determine whether coronary segment visibility was similar in group 1 and group 2 or superior on one series of images.

Conditions of image analysis

Two cardiothoracic pediatric radiologists, A.B. with 4 years and J.-B.F. with 7 years of experience in chest and cardiac CT, who were blinded to clinical and reconstruction data, independently reviewed anonymized transverse CT images to grade coronary artery visibility. Each reader analyzed separately and in random order group 1 and group 2 images. Multiplanar reformations and maximum-intensity projection could be used to assess coronary segment visibility at the reader's discretion. In a separate session, each reader compared the visibility of each coronary segment between group 1 and group 2 images; this analysis was based on the simultaneous reading of paired images.

Statistical analysis

Statistical analyses were performed using the SAS software (SAS Institute, Cary, NC). Results were expressed as means and standard deviations (SD) for quantitative variables, and frequencies and percentages for categorical variables. The level of agreement between the readers in visual grading of coronary artery visibility was analyzed by the kappa coefficients; kappa values were interpreted as follows: <0, no agreement; 0.0–0.20, slight agreement; 0.21–0.40, fair agreement; 0.41–0.60, moderate agreement; 0.61–0.80, substantial agreement; 0.81–1.00, almost perfect agreement [16]. Grades of coronary

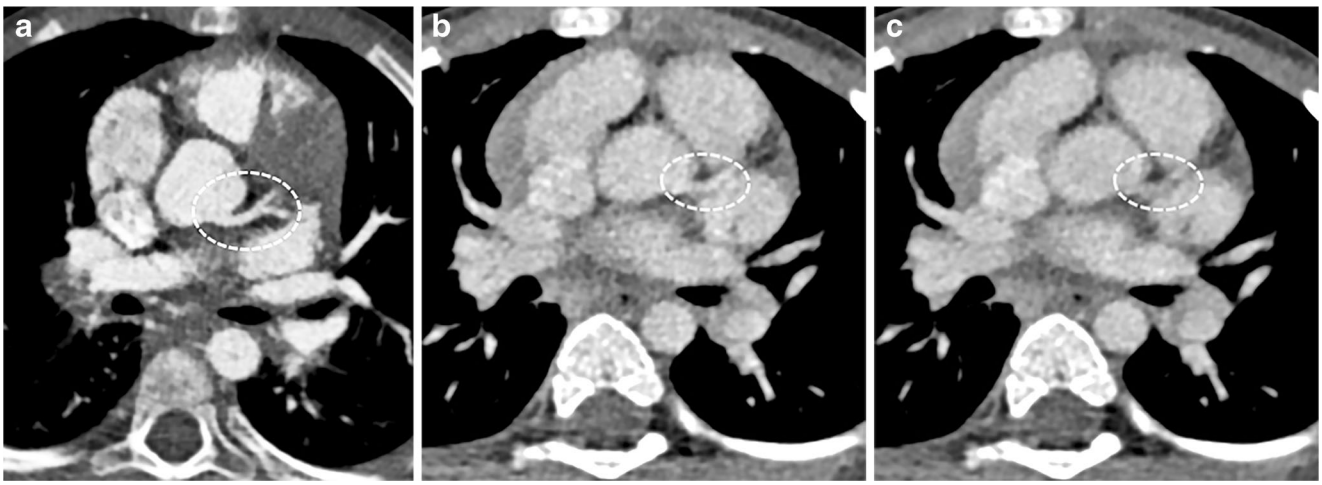

Fig. 1 Comparison of the image quality of grades 3, 4 and 5, all levels at which a coronary segment was detected, on CT angiographic images. Grades 1 and 2 are not shown; in these the coronary segment was poorly visualized. **a** Grade 5. There is clear delineation of the left main coronary artery (*dashed circle*) without any motion artifact. This grade provides excellent diagnostic confidence. **b** Grade 4. There is clear delineation of the left main coronary artery (*dashed circle*) with mild motion artifacts. This grade provides high diagnostic confidence. **c** Grade 3. There is visualization of the left main coronary artery (*dashed circle*) with blurring motion artifacts. The coronary segment is identified with moderate diagnostic confidence

artery visibility and percentages of segments with a grade ≥3 were compared between group 1 and group 2 by the McNemar test. The objective evaluation of image quality was tested between group 1 and group 2 by the paired Student's *t*-test; the grades of visibility of coronary segments between the groups were compared using the paired Wilcoxon test. Statistical significance was defined as $P<0.05$.

Results

Characteristics of data acquisition and objective image quality in groups 1 and 2

During a 2-year period (July 2011 to June 2013), 107 consecutive children were eligible for inclusion in this study; 14 children were excluded because raw datasets could not be reconstructed at the time of our research analysis. In the remaining 93 children, chest CT angiography was indicated for bronchopulmonary anomalies ($n=38$), anomalies of the pulmonary arteries, pulmonary veins or aortic arch ($n=24$), acquired bronchopulmonary disease ($n=18$), suspicion of pulmonary embolism ($n=8$), cystic fibrosis ($n=3$) and esophageal atresia ($n=2$).

The study population comprised 58 boys and 35 girls, including 8 newborns, 56 infants and 29 children ages 1–4 years. The mean (SD) weight of the study population was 7.73 (3.84) kg. Table 1 summarizes the characteristics of data acquisitions in the study population. Objective image quality of group 1 and group 2 images is summarized in Table 2, which shows significantly higher noise and lower signal-to-noise ratio in group 1 compared to group 2 images.

Detection rate of coronary segments in groups 1 and 2 (Table 3)

We analyzed a total of 558 proximal and mid-coronary segments. The interobserver agreement in assessing coronary artery visibility was found to be almost perfect (group 1: kappa value of 0.86 [95% confidence intervals: 0.83–0.90]; group 2: 0.86 [95% confidence intervals: 0.82–0.89]). Intergroup comparisons were subsequently based on the most experienced reader's results.

Table 1 Characteristics of data acquisitions in the study population ($n=93$)

z-axis coverage, *mm* mean±SD (range)	150.60±29.49 (92–247)
Duration of data acquisition, *s* mean±SD (range)	0.56±0.10 (0.34–0.92)
Dose-length product (32-cm phantom), *mGy cm* mean±SD (range)	16.76±2.74 (8–26)
CT dose index volume ($CTDI_{vol}$), *mGy* mean±SD (range)	0.78±0.09 (0.46–1.45)
Age-adjusted effective dose, *mSv* mean±SD (range)	0.92±0.27 (0.54–2.03)

SD standard deviation

Table 2 Objective evaluation of image quality of group 1 and group 2 images

	Group 1 *75 ms*	Group 2 *140 ms*	*P*–value*
Aorta			
Noise, *HU* mean±SD	27.14±6.96	22.78±5.91	<0.0001
Attenuation, *HU* mean±SD	333.68±86.99	328.51±84.38	0.01
Signal-to-noise ratio mean±SD	12.75±3.39	14.96±4.19	<0.0001
Pulmonary trunk			
Noise, *HU* mean±SD	25.80±6.28	20.92±4.57	<0.0001
Attenuation, *HU* mean±SD	290.46±70.54	285.64±65.26	0.008
Signal-to-noise ratio mean±SD	11.63±2.94	14.04±.45	<0.0001

*Comparisons of group 1 and group 2 results were obtained using the paired Student's *t*-test

SD standard deviation

The percentage of coronary segments rated as detected (grade ≥3) was significantly higher in group 1 than in group 2 (Table 3) when considering all segments and proximal segments alone; there was no statistically significant difference for mid-segments between the groups.

Table 4 provides detailed analysis of the rate of detection of proximal segments according to the anatomical sites, ranging 11–64.5% in group 1 and 10–58% in group 2. In both groups, the highest rates of detection were observed for the left main coronary artery (S1) (group 1: 64.5%; group 2: 58.1%) and proximal left anterior descending artery (S2) (group 1: 43.0%; group 2: 41.9%). Significantly higher rates of detection were seen in group 1 for the left main coronary artery (S1) ($P=0.0339$), proximal right coronary artery (S7) ($P=0.0114$), proximal segments of the left coronary artery (S1+S2+S5) ($P=0.0209$) and proximal segments of the left and right coronary arteries ($P=0.0006$). The detection rates of the proximal left anterior descending artery (S2) and left circumflex artery (S5) did not differ between the groups.

Grades of visibility of proximal coronary segments in groups 1 and 2 (Table 5)

The mean grade of visibility was significantly higher in group 1 than in group 2 for the left main coronary artery (S1), proximal right coronary artery (S7) and proximal segments of the right and left coronary arteries. In group 1, the mean

Table 3 Overall rates of detection of coronary segments in group 1 and group 2

	Rate of detection		
	Group 1 *75 ms*	Group 2 *140 ms*	*P*-value*
All segments (*n*=558)	27.2% (152/558) *(95% CI: 23.6–31.1)*	24.2% (135/558) *(95% CI: 20.7–27.9)*	0.0004
Proximal segments *(S1,S2,S5,S7)* (*n*=372)	36.5% (136/372) *(95% CI: 31.6 – 41.7)*	32.3% (120/372) *(95% CI: 27.5–37.3)*	0.0006
Middle segments *(S3,S8)* (*n*=186)	8.6% (16/186) *(95% CI: 4.9–13.6)*	8.1% (15/186) *(95% CI: 4.6–12.9)*	0.3

*Comparisons of group 1 and group 2 results were obtained using the McNemar test

CI confidence interval

grades of visibility were 1.9 for proximal right coronary artery (S7), 2.7 for the left main coronary artery (S1) and 2.0 for the proximal segments of the right and left coronary arteries (S1+S2+S5+S7).

Simultaneous analysis of proximal segments on paired images of groups 1 and 2 (Table 6)

Except for the left main coronary artery, the visibility of proximal coronary segments that was found to be equivalent on group 1 and group 2 images ranged 57–63%. When differences were depicted between group 1 and group 2 images, there was a superior visibility of proximal coronary segments on group 1 images in 92–97% of cases (Figs. 2, 3 and 4).

Discussion

To our knowledge, this is the first study to investigate the impact of temporal resolution on the visibility of coronary arteries on non-ECG-gated, high-pitch dual-source CT examinations. The originality of our study design relied on the possibility of generating two series of images from each dataset, thus allowing comparison of coronary artery visibility in strictly similar conditions for each child with the exception of the temporal resolution (Fig. 5). Although this technical approach can be theoretically applied to single-source CT systems, achieving a temporal resolution of 75 ms is beyond the capabilities of these systems. For single-source CT systems, the best possible temporal resolution is half the rotation time, and the fastest rotation time is 0.28 s, thus leading to a tem-

Table 4 Rate of detection of proximal coronary segments according to the anatomical sites in groups 1 and 2

	Rate of detection		
	Group 1 *75 ms*	Group 2 *140 ms*	*P*-value*
Left main coronary artery *(S1)* (*n*=93)	64.5% (60/93) *(95% CI: 53.9–74.2)*	58.1% (54/93) *(95% CI: 47.4 – 68.2)*	0.03
Proximal segment of left anterior descending artery *(S2)* (*n*=93)	43.0% (40/93) *(95% CI: 32.8–53.7)*	41.9% (39/93) *(95% CI: 31.8–52.6)*	0.6
Proximal segment of left circumflex artery *(S5)* (*n*=93)	10.8% (10/93) *(95% CI: 5.3–18.9)*	9.7% (9/93) *(95% CI: 4.5–17.6)*	0.3
Proximal segment of right coronary artery *(S7)* (*n*=93)	28.0% (26/93) *(95% CI: 19.1–38.2)*	19.4% (18/93) *(95% CI: 11.9–28.9)*	0.01
Proximal segments of the left coronary artery *(S1+S2+S5)* (*n*=279)	39.4% (110/279) *(95% CI: 33.6–45.4)*	36.6% (102/279) *(95% CI: 30.9–42.5)*	0.02
Proximal segments of the right and left coronary arteries *(S1+S2+S5+S7)* (*n*=372)	36.6% (136/372) *(95% CI: 31.6–41.7)*	32.3% (120/372) *(95% CI: 27.5–37.3)*	0.0006

*Comparisons of group 1 and group 2 results were obtained using the McNemar test

CI confidence interval

Table 5 Grades (mean±standard deviation) of visibility of proximal coronary segments in groups 1 and 2

	Grades of visibility mean±SD		
	Group 1 *75 ms*	Group 2 *140 ms*	*P*-value*
Left main coronary artery *(S1)* (*n*=93)	2.65±0.83	2.56±0.84	0.0215
Proximal segment of left anterior descending artery *(S2)* (*n*=93)	2.18±0.86	2.13±0.89	0.1250
Proximal segment of left circumflex artery *(S5)* (*n*=93)	1.41±0.68	1.37±0.66	0.1250
Proximal segment of right coronary artery *(S7)* (*n*=93)	1.91±0.90	1.76±0.84	0.0005
Proximal segments of the left coronary artery *(S1+S2+S5)* (*n*=279)	2.08±0.94	2.02±0.94	<0.0001
Proximal segments of the right and left coronary arteries *(S1+S2+S5+S7)* (*n*=372)	2.04±0.93	1.95±0.92	<0.0001

*Comparisons of group 1 and group 2 results were obtained using the paired Wilcoxon test *SD* standard deviation

poral resolution of 140 ms. To achieve a temporal resolution of 75 ms, a rotation time of 0.15 s would be needed, and that cannot be reached with a single-source volume scanner. In group 1 it was possible to evaluate the rate of detection of coronary arteries with the optimized temporal resolution of a second-generation dual-source CT system, i.e. 75 ms. These results could then be compared to group 2 results, which were based on images acquired with a temporal resolution of 140 ms that can be assimilated to the optimized temporal resolution (TR) on single-source CT systems [17]. In free-breathing young children, the rate of detection of proximal segments of the right and left coronary arteries was significantly higher in group 1 than in group 2, whereas there was no significant difference for mid-segments. When analyzing proximal segments according to the anatomical sites, the rates of detection were significantly higher for the left main coronary artery and proximal right coronary artery while there were no significant differences between the groups for the

Table 6 Comparison of proportions of visibility of the proximal coronary segments with techniques 1 (temporal resolution: 75 ms) and 2 (temporal resolution: 140 ms)

	Similar	One technique superior
Left main coronary artery *(S1)* (*n*=93)	30.1% *(28/93)*	69.9% *(65/93)* -Group 1 superiority: 60/65 *(92.3%)* -Group 2 superiority: 5/65 *(8.7%)*
Proximal segment of the right coronary artery *(S7)* (*n*=93)	63.4% *(59/93)*	36.6% *(34/93)* -Group 1 superiority: 33/34 *(97.1%)* -Group 2 superiority: 1/34 *(2.9%)*
Proximal segments of the left coronary artery *(S1+S2+S5)* (*n*=279)	56.6% *(158/279)*	43.4% *(121/279)* -Group 1 superiority: 112/121 *(92.6%)* -Group 2 superiority: 9/121 *(7.4%)*
Proximal segments of the right and left coronary arteries *(S1+S2+S5+S7)* (*n*=372)	58.3% *(217/372)*	41.7% *(155/372)* - Group 1 superiority: 145/155 *(93.5%)* - Group 2 superiority: 10/155 *(6.5%)*

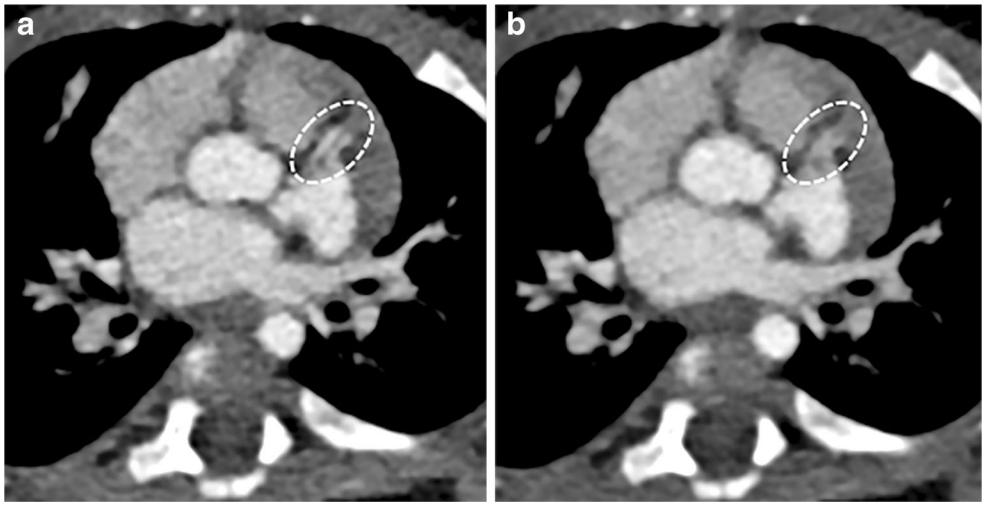

Fig. 2 Chest CT angiogram obtained in a 1-year-old boy to rule out bronchopulmonary malformation illustrates the influence of temporal resolution on the visibility of the proximal segment of the left anterior descending coronary artery (S2). **a** Group 1 axial CT image at the level of the left inferior pulmonary vein (75 ms temporal resolution). S2 (medial) is seen with mild motion artifact, clearly distinguished from the great cardiac vein (lateral) (*dashed circle*); S2 was rated with a grade 4 visibility. **b** Group 2 axial CT image obtained at the same level as that seen in (**a**) (140 ms temporal resolution). S2 cannot be distinguished from the great cardiac vein (*dashed circle*); S2 was rated with a grade 2 visibility

proximal left anterior descending artery and proximal left circumflex artery. Higher rates of detection were also observed in group 1 when considering the proximal segments of the left coronary artery and the proximal segments of the right and left coronary arteries. The superiority of group 1 results was observed despite lower image quality compared to group 2 images. In group 1, the mean level of noise was significantly higher than that of group 2, related to the fact that only part of the available data per image was used for image reconstruction. Moreover, group 1 images were also characterized by a lower signal-to-noise ratio. However, the signal-to-noise ratio was in the range of that reported in pediatric high-pitch cardiovascular CT angiography using manual (hand) injection [18], which could be related to the low kilovoltage used to scan our population.

In group 1, 64.4% of left main coronary arteries were detectable but the rate of detection dropped to 28.0% for the proximal right coronary artery. Regarding the visibility of proximal segments of both coronary arteries, it was found achievable in 36.5% of cases. These results are encouraging but are obviously inferior to those achievable on ECG-gated examinations. Based on prospective or retrospective ECG

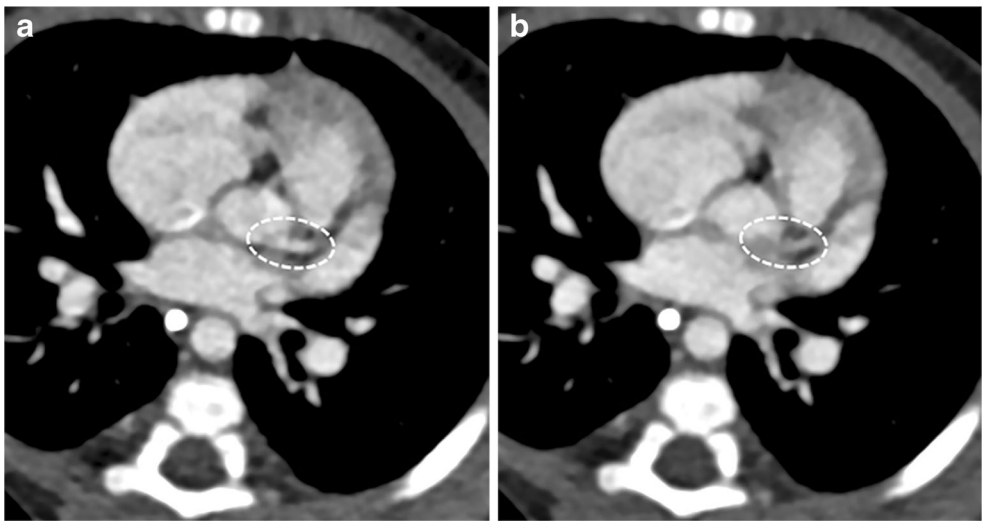

Fig. 3 Chest CT angiogram obtained in a 6-month-old boy to rule out congenital bronchopulmonary malformation illustrates the influence of temporal resolution on visibility of the left main coronary artery (S1). **a** Group 1 axial CT image at the level of the inferior pulmonary veins (75 ms temporal resolution). S1 (*dashed circle*) is more clearly delineated and was rated with a grade 3 visibility. **b** Group 2 axial CT image obtained at the same level as that seen in (**a**) (140 ms temporal resolution). The origin of the left main coronary artery (*dashed circle*) cannot be clearly separated from the anterior border of the left atrium. In this image, S1 was rated with a grade 2 visibility

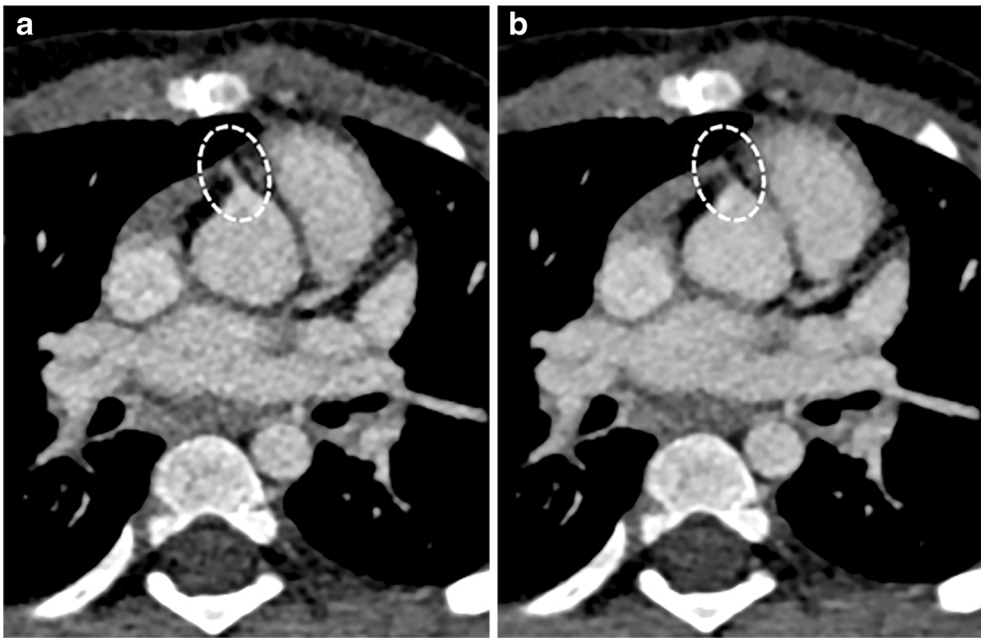

Fig. 4 Chest CT angiogram in a 2-year-old boy to rule out aortic arch anomaly illustrates the influence of temporal resolution on the visibility of the proximal segment of the right coronary artery (S7). **a** Group 1 axial CT image at the level of the superior pulmonary veins (75 ms temporal resolution). S7 (*dashed circle*) is detected with mild motion artifact. In this image S7 was rated with a grade 4 visibility. **b** Group 2 axial CT image obtained at the same level as that seen in (**a**) (140 ms temporal resolution). A faint opacified structure (*dashed circle*) is identified but equivocal. S7 was rated with a grade 2 visibility

gating, coronary artery visualization was reported to vary in 70–100% of cases [12–15, 19]. However, imaging of coronary arteries without ECG synchronization in pediatric populations is challenging because of the conjunction of several anatomical and physiological parameters. Based on echocardiographic and angiographic findings, the diameter of the proximal coronary arteries was reported to vary from 1 mm in newborns to <3 mm in 4-year-olds [20, 21]. The velocity of the coronary arterial movement in the transverse plane also has important implications for coronary artery imaging. In a recent study, Farshad-Amacker and coworkers [22] demonstrated that high-pitch dual-source CT acquisition compensates for motion artifacts of moving objects up to 2 cm/s in various directions during acquisition. The velocity of coronary arteries in young children is much higher than this threshold. In adults with a mean heart rate of 71 bpm, Achenbach et al. [23] demonstrated that the mean velocity of coronary arteries was 46.6 mm/s. Considering the higher heart rates of young children and the relationships between heart rate and coronary artery motion [24], it is likely that cardiac motion has a greater impact on the sharpness of proximal coronary artery imaging in children. Although ECG-triggered acquisitions are the standard of reference for evaluating complex anatomy of congenital heart disease [12, 25, 26], high-pitch multidetector CT angiography imaging has recently been found to be the preferred mode of imaging for specific subsets of children for the definition of combined cardiac and extracardiac anatomy [4, 11]. Were coronary arteries assessable in these scanning

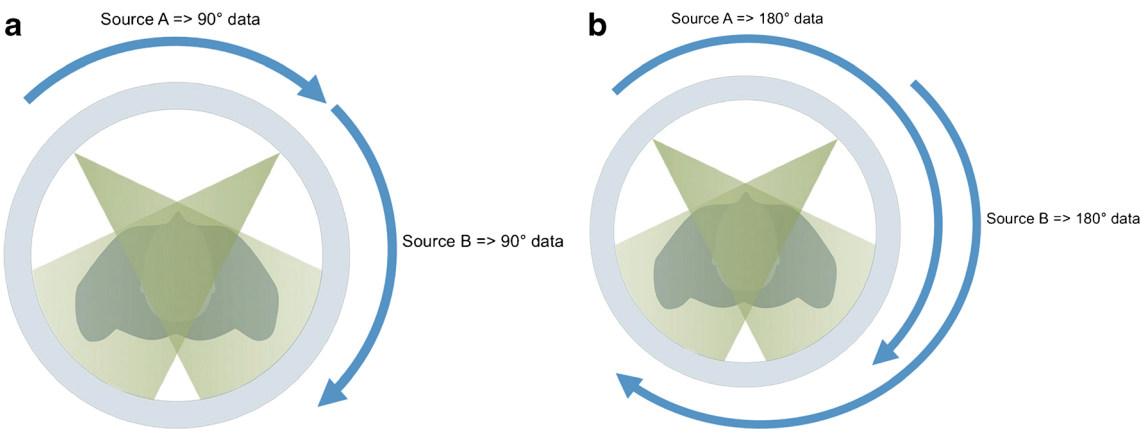

Fig. 5 Illustration shows the influence of the reconstruction algorithm on temporal resolution. **a** With the half-scan reconstruction algorithm, acquisition of only 180° of data is necessary for one cross-sectional image. There are no redundant data. Because the dual-source CT system uses two X-ray tubes and two detectors arranged at an angle of 90°, the temporal resolution is optimized to one-quarter of the gantry rotation time. **b** With the standard reconstruction algorithm, 180° of data are acquired by each source. There are redundant data. Temporal resolution is limited to half-gantry rotation time

conditions, coronary artery anomalies could be detected, particularly malignant forms, which could be seen as unique findings in asymptomatic children [27, 28]. An optimized temporal resolution should benefit visualization of not only cardiovascular structures but also structural changes at the level of airways and within the lung parenchyma [29].

We acknowledge several limitations of this study. First, we did not rate the overall image quality and focused our analysis on coronary artery visibility. However, all examinations were judged as fully diagnostic in the conditions of routine clinical activity. Second, group 1 images were acquired with a pitch of 2.0 whereas a pitch of 3.0 corresponds to optimized high-pitch examinations. This parameter was chosen owing to the overranging effects of high-pitch selections on small children [4, 30]. Using a dual-source CT scanner, the pitch could be increased to a maximum value of 3.2, but this would not have changed the temporal resolution, which was kept at 75 ms. A further increase of the pitch (with a potentially further improved temporal resolution) is not possible. In such a situation, no complete data along the child's longitudinal axis are acquired, leading to data gaps and thus to artifacts in the images. Third, we did not investigate specifically respiratory motion artifacts. As previously reported by Lell et al. [4], all children were scanned in high-pitch mode, which is known to provide the highest image quality, making sedation or controlled ventilation for the examinations of infants, small or uncooperative children unnecessary. Last, we did not provide information on the children's heart rates. However, neonates and young children are characterized by high resting heart rates [31, 32].

Conclusion

The study demonstrated that a temporal resolution of 75 ms significantly improved the detection of coronary arteries compared to that achievable with a 140-ms temporal resolution.

Conflicts of interest Dr. Flohr is a Siemens employee who provided the research prototype enabling reconstruction of images with different temporal resolutions. His professional position had no influence on the results of this investigation, which was independently conducted by the radiologic and statistical departments of our university center.

Appendix

We reconstructed two sets of CT images from the same CT raw data, one with the standard reconstruction implemented on the dual-source CT scanner, the other with an off-line reconstruction using optimized temporal resolution, running on a separate PC.

For image reconstruction of the dual-source CT data acquired at pitch 2, an angular range of 180° of CT raw data per measurement system (in parallel geometry) are available for each image close to the isocenter of the CT scanner [33]. In the standard filtered back-projection reconstruction as well as when using the iterative reconstruction SAFIRE, all scan data available per image contribute to the final image, i.e. the full angular range of 180°. This type of image reconstruction, which we used to generate the first set of CT images, is beneficial for complete utilization of the applied radiation dose, but it is suboptimal with regard to temporal resolution. A scan data range of 180° corresponds to a temporal resolution of 140 ms at 0.28-s gantry rotation time. We obtained the second set of images with an alternative off-line reconstruction that uses only the minimum scan data range of 90° (in parallel geometry) per measurement system for each image. By doing so, only a sub-range of the available CT data contributes to each image. This approach is suboptimal with regard to dose utilization, but it provides images with the best possible temporal resolution of 75 ms. The method is fully equivalent to the image reconstruction that would have been used on the scanner if the scan data had been acquired at a higher pitch of 3.2. Reconstruction of both image datasets allows for an assessment of the effect of improved temporal resolution on the analyzability of coronary arteries.

References

1. Petersilka M, Bruder H, Krauss B et al (2008) Technical principles of dual source CT. Eur J Radiol 68:362–368
2. Tacelli N, Remy-Jardin M, Flohr T et al (2010) Dual-source chest CT angiography with high temporal resolution and high pitch modes: evaluation of image quality in 140 patients. Eur Radiol 20:1188–1196
3. Schultz B, Jacobi V, Beeres M et al (2012) Quantitative analysis of motion artifacts in high-pitch dual-source computed tomography of the thorax. J Thorac Imaging 27:382–386
4. Lell MM, May M, Deak P et al (2011) High-pitch spiral computed tomography: effect on image quality and radiation dose in pediatric chest computed tomography. Investig Radiol 46:116–123
5. Karlo C, Leschka S, Goetti RP et al (2011) High-pitch dual-source CT angiography of the aortic valve-aortic root complex without ECG-synchronization. Eur Radiol 21:205–212
6. Budoff MJ, Nasir K, Kinney GL et al (2011) Coronary artery and thoracic calcium on noncontrast thoracic CT scans: comparison of ungated and gated examinations in patients from the COPD gene cohort. J Cardiovasc Comput Tomogr 5:113–118
7. Beeres M, Schell B, Mastragelopoulos A et al (2012) High-pitch dual-source CT angiography of the whole aorta without ECG synchronization: initial experience. Eur Radiol 22:129–137
8. De Malherbe M, Duhamel A, Tacelli N et al (2012) Ultrafast imaging of the entire chest without ECG synchronization or beta-blockade: to what extent can we analyze the coronary arteries. Insights Imaging 3:73–79
9. Liu Y, Xu J, Li J et al (2013) The ascending aortic image quality and the whole aortic radiation dose of high-pitch dual-source CT angiography. J Cardiothorac Surg 8:228–232

10. Nakagawa J, Tasaki O, Watanabe Y et al (2013) Reduction of thoracic aorta motion artifact with high-pitch 128-slice dual-source computed tomographic angiography: a historical control study. J Comput Assist Tomogr 37:755–759
11. Han BK, Lindberg J, Grant K et al (2011) Accuracy and safety of high pitch computed tomography imaging in young children with complex congenital heart disease. Am J Cardiol 107:1541–1546
12. Paul JF, Rohnean A, Elfassy E et al (2011) Radiation dose for thoracic and coronary step-and-shoot CT using a 128-slice dual-source machine in infants and small children with congenital heart disease. Pediatr Radiol 41:244–249
13. Nie P, Wang X, Cheng Z et al (2012) Accuracy, image quality and radiation dose comparison of high-pitch spiral and sequential acquisition on 128-slice dual-source CT angiography in children with congenital heart disease. Eur Radiol 22:2057–2066
14. Tsai IC, Lee T, Chen MC et al (2007) Visualization of neonatal coronary arteries on multidetector row CT: ECG-gated versus non-ECG-gated technique. Pediatr Radiol 37:818–825
15. Ben Saad M, Rohnean A, Sigal-Cinqualbre A et al (2009) Evaluation of image quality and radiation dose of thoracic and coronary dual-source CT in 110 infants with congenital heart disease. Pediatr Radiol 39:668–676
16. Landis JR, Koch GG (1977) The measurement of interobserver agreement for categorical data. Biometrics 33:159–174
17. Rogalla P, Kloeters C, Hein PA (2009) CT technology overview: 64-slice and beyond. Radiol Clin N Am 47:1–11
18. Saake M, Lell MM, Rompel O et al (2014) Contrast medium application in pediatric high-pitch cardiovascular CT angiography: manual or power injector? J Cardiovasc Comput Tomogr 8:315–322
19. Goo HW, Yang DH (2010) Coronary artery visibility in free-breathing young children with congenital heart disease on cardiac 64-slice CT: dual-source ECG-triggered sequential scan vs. single-source non-ECG-synchronized spiral scan. Pediatr Radiol 40: 1670–1680
20. Oberhoffer R, Lang D, Feilen K (1989) The diameter of coronary arteries in infants and children without heart disease. Eur J Pediatr 148:389–392
21. Arjunan K, Daniels SR, Meyer RA et al (1986) Coronary artery caliber in normal children and patients with Kawasaki disease but without aneurysms: an echocardiographic and angiographic study. J Am Coll Cardiol 8:1119–1124
22. Farshad-Amacker NA, Alkhadi H, Leschka S et al (2013) Effect of high-pitch dual-source CT to compensate motion artifacts: a phantom study. Acad Radiol 20:1234–1239
23. Achenbach S, Ropers D, Holle J et al (2000) In-plane coronary arterial motion velocity: measurement with electron-beam CT. Radiology 216:457–463
24. Husmann L, Leschka S, Desbiolles L et al (2007) Coronary artery motion and cardiac phases: dependency on heart rate — implications for CT image reconstruction. Radiology 245:567–576
25. Gao Y, Lu B, Hou Z et al (2012) Low-dose dual-source CT angiography in infants with complex congenital heart disease: a randomized study. Eur J Radiol 81:e789–e795
26. Klink T, Müller G, Weil J et al (2012) Cardiovascular computed tomography angiography in newborns and infants with suspected congenital heart disease: retrospective evaluation of low-dose scan protocols. Clin Imaging 36:746–753
27. Shi H, Aschoff AJ, Brambs HJ et al (2004) Multislice CT imaging of anomalous coronary arteries. Eur Radiol 14:2172–2181
28. Van Ooijen PMA, Dorgelo J, Zijlstra F et al (2004) Detection, visualization and evaluation of anomalous coronary artery anatomy on 16-slice multidetector-row CT. Eur Radiol 14:2163–2171
29. Young C, Xie C, Owens CM (2012) Paediatric multidetector row chest CT: what you really need to know. Insights Imaging 3:229–246
30. Nievelstein RAJ, van Dam IM, van der Molen AJ (2010) Multidetector CT in children: current concepts and dose reduction strategies. Pediatr Radiol 40:1324–1344
31. Davignon A, Rautahrju P, Boisselle E et al (1979) Normal ECG standards for infants and children. Pediatr Cardiol 1:123–131
32. Rijnbeek PR, Witsenburg M, Schrama E et al (2001) New normal limits for the paediatric electrocardiogram. Eur Heart J 22: 702–711
33. Flohr TG, Leng S, Yu L et al (2009) Dual-source spiral CT with pitch up to 3.2 and 75 ms temporal resolution: image reconstruction and assessment of image quality. Med Phys 36:5641–5653